Synchrosqueezed Wavelet Transform for Damping Identification

Marko Mihalec, Janko Slavič, Miha Boltežar
University of Ljubljana, Faculty of Mechanical Engineering,
Aškerčeva 6, Ljubljana, Slovenia

May 16, 2016

Cite as:
Marko Mihalec, Janko Slavič and Miha Boltežar,
Synchrosqueezed Wavelet Transform for Damping Identification,
Mechanical Systems and Signal Processing (2016),
10.1016/j.ymssp.2016.05.005.

Abstract

Synchrosqueezing is a procedure for improving the frequency localization of a continuous wavelet transform. This research focuses on using a synchrosqueezed wavelet transform (SWT) to determine the damping ratios of a vibrating system using a free-response signal. While synchrosqueezing is advantageous due to its localisation in the frequency, damping identification with the original SWT is not sufficiently accurate. Here, the synchrosqueezing was researched in detail, and it was found that an error in the frequency occurs as a consequence of the numerical calculation of the preliminary frequencies. If this error were to be compensated, a better damping identification would be expected. To minimize the frequency-shift error, three different strategies are investigated: the scale-dependent coefficient method, the shifted-coefficient method and the autocorrelated-frequency method. Furthermore, to improve the SWT, two synchrosqueezing criteria are introduced: the average SWT and the proportional SWT. Finally, the proposed modifications are tested against close modes and the noise in the signals. It was numerically and experimentally confirmed that the SWT with the proportional criterion offers better frequency localization and performs better than the continuous wavelet transform when tested against noisy signals.

1 Introduction

Damping is a mechanism that is present in every real vibrating structure. It originates as a combination of external factors, the properties of a structure and from the material itself. Identifying the damping together with identifying the natural frequencies is a key element in the characterization of a system.

The continuous wavelet transform (CWT) has been used as a tool for damping identification and has proven to be very useful, even for noisy signals [1, 2, 3, 4]. For the extraction of the modal parameters, the CWT has been continuously studied and improved, e.g., with the introduction of the Gabor wavelet [5], and studies of the edge-effect and time-frequency localization [6, 7]. To improve the damping identification, different methods related to the CWT have been proposed, e.g., [8]. The CWT is being used for the damping identification in various different applications, e.g., on bladed disks [9], the damping of bridges [10] and in ocean engineering [11].

In order to improve the wavelet transform, synchrosqueezing has recently been proposed [12, 13]. Synchrosqueezing adds to an existing transform by examining the local oscillations with respect to time. Based on this, synchrosqueezing re-allocates each value of the original transform to a new frequency on the time-frequency plane. The resulting time-frequency representation is thus sharpened in the frequency domain.

The synchrosqueezed wavelet transform (SWT) aims to combine the advantages of the CWT with the sharpening provided by the synchrosqueezing; it has been applied to a variety of different problems, often in the field of medicine [12], but also in the field of seismology [14].

In the field of mechanical engineering, the SWT has been introduced for the fault diagnosis of gearboxes [15, 16, 17]. Recently, generalized synchrosqueezed transforms have been introduced for bearings defects detection and diagnosis [18, 19]. A comparison between the wavelet transform and its synchrosqueezed version was made in [20], where according to the authors, more visually appealing pictures appear to be the only advantage of synchrosqueezing. The synchrosqueezed wavelet transform has also been used for damping identification [21], being applied to seismic signals, where it has been compared to the wavelet and Hilbert-Huang transforms. It was found that although the SWT produces sharper representations, when identifying damping, it is less stable than the CWT-based approach.

In Section 2, the theoretical background to the continuous wavelet transform and synchrosqueezing are presented, followed by a method for damping identification based on the logarithmic decay of the envelope. In Section 3,

some sources of error in the identification of damping with synchrosqueezing are addressed. The next Section explores the effects of synchrosqueezing on signals with closely spaced modes. Section 5 focuses on the use of the SWT for damping identification. For better results, two modifications are proposed. Section 6 offers numerical experiments as well as an application involving real data. The last section draws the conclusions.

2 Theoretical background

In order α to perform a wavelet transform, a mother wavelet function $\psi(t)$ is needed. According to Mallat [22], such a function must have a zero mean value Eq. (1) and has to be normalized Eq. (2).

$$\int_{-\infty}^{+\infty} \psi(t)\ \mathrm{d}t = 0 \tag{1}$$

$$\|\psi(t)\|^2 = \int_{-\infty}^{+\infty} |\psi(t)|^2 \mathrm{d}t = 1 \tag{2}$$

The wavelet function $\psi(t)$ has to be translated in time by u and scaled by $s > 0$ to obtain a family of wavelet functions $\psi_{u,s}(t)$:

$$\psi_{u,s}(t) = \frac{1}{\sqrt{s}}\,\psi\left(\frac{t-u}{s}\right). \tag{3}$$

The continuous wavelet transform of a function $x(t)$ can now be defined as:

$$Wx(u,s) = \int_{-\infty}^{+\infty} x(t)\ \psi^*_{u,s}(t)\mathrm{d}t, \tag{4}$$

where $\psi^*_{u,s}(t)$ denotes a complex conjugate of the wavelet $\psi_{u,s}(t)$. The scale s and the angular velocity $\omega(s)$ are related via the frequency modulation η as: $\omega(s) = \eta/s$.

In this paper, the Gabor wavelet will be used:

$$\psi_{Gabor}(t) = \frac{1}{(\sigma^2\,\pi)^{1/4}} \mathrm{e}^{-t^2/(2\sigma^2)}\,\mathrm{e}^{\mathrm{i}\,\eta\,t}. \tag{5}$$

The parameter σ denotes the width of the Gaussian window of the Gabor wavelet. If $\sigma = 1$ is chosen, the Gabor wavelet becomes identical to the Morlet wavelet. Choosing appropriate values for the parameters σ and η is critical to the transform; they have to be small enough to reduce the edge effect and the time spread, yet large enough to reduce the frequency spread.

Synchrosqueezing, as defined by Daubechies et al. [12], requires three steps. The first step is to calculate a CWT for the (discrete) time u and the (discrete) scale s according to Eq. (4). In the second step, a preliminary frequency $\omega(u, s)$ is obtained from the oscillatory behaviour of $Wx(u, s)$ in u:

$$\omega(u, s) = -\mathrm{i}(Wx(u, s))^{-1} \frac{\partial}{\partial u} Wx(u, s). \tag{6}$$

In the third step the information is transformed from the time-scale plane to the time-frequency plane. Each value of $Wx(u, s)$ is re-assigned to (u, ω_l), where ω_l is the frequency that is the closest to the preliminary frequency of the original (discrete) point $\omega(u, s)$. This is formally written in Eq. (7):

$$T(u, \omega_l) = (\Delta\omega)^{-1} \sum_{s_k : |\omega(u,s_k) - \omega_l| \leq \Delta\omega/2} Wx(u, s_k)\, s_k^{-3/2} \Delta s, \tag{7}$$

where $\Delta\omega$ denotes the width of each frequency bin $\Delta\omega = \omega_l - \omega_{l-1}$ and equivalently for $\Delta s = s_k - s_{k-1}$.

2.1 Damping identification

For a MDOF system, where N denotes the number of modes, an impulse response can be given as the sum of the responses for each mode:

$$x(t) = \sum_{i=1}^{N} A_{0,i} \mathrm{e}^{-\zeta_i \omega_{0,i} t} \cos(\omega_{0,i} \sqrt{(1 - \zeta_i^2)}\, t + \varphi_i), \tag{8}$$

where ζ_i is the damping ratio of the i-th mode, $\omega_{0,i}$ is the natural angular velocity, $A_{0,i}$ is the i-th mode's magnitude and φ_i is the phase shift. From a given signal, it is only possible to obtain the damped angular velocity $\omega_{di} = \omega_{0,i}\sqrt{1 - \zeta^2}$. Since the ζ is usually very small, the natural and the damped angular frequency are very close, so they can be substituted. Instead of solving the whole MDOF system at once, it can be decoupled into single modes, so each i-th part of Eq. (8) can be solved separately. As shown by Staszewski [1] for the Morlet wavelet and adopted in [5] for the Gabor wavelet, the damping ratio can be estimated from the slope of a semi-logarithmic plot as:

$$\ln\left(\frac{2|Wx(u, s(u))|}{(4\pi\, \sigma^2\, s(u)^{1/4}}\right) \approx -\zeta\, \omega_d\, u + \ln(A_0). \tag{9}$$

where $s(u)$ in Eq. (9) denotes the ridge. The ridge is a curve in (u, s) that follows the local maxima of wavelet transform modulus at each u. The values that correspond to the ridge are called the skeleton and are denoted

as $Wx(u, s(u))$. Different approaches to ridge detection have been introduced [23, 1], which are based on amplitude, phase or the shape of the ridge. Because the SWT uses the phase information to rearrange the coefficients and can thereby slightly change the shape of the ridge, a simple amplitude method which searches for the local maximum of a transform was used in this study.

A similar approach as that developed for damping identification using the CWT will be applied here for the damping identification using the synchrosqueezed CWT. It must be noted that when applied to the synchrosqueezed CWT, the last part of Eq. (9) is no longer equal to $\ln(A_0)$.

3 Frequency shift

After synchrosqueezing a CWT, the extreme of the amplitude might shift to lower frequencies. This shift is dependent on the time discretization and originates in a numerical calculation of the preliminary frequencies in Equation (6). This section will present the mathematical background and the limits for such a frequency shift, as well as three methods for its reduction.

Let us assume a harmonic signal with a constant amplitude A_0 and a constant angular frequency ω_0:

$$x(t) = A_0 \cos(\omega_0 t) \tag{10}$$

It has been shown [5] that for this kind of signal the CWT can be calculated analytically. Focusing on the translation u the analytically defined CWT is:

$$Wx(u) = K\mathrm{e}^{-\mathrm{i}u\omega_0} \tag{11}$$

where K is a constant in time, dependent on the scale $K = K(s)$. The same equation can also be written as the sum of the real and imaginary components as:

$$Wx(u) = K\cos(u\,\omega_0) - \mathrm{i}K\sin(u\,\omega_0). \tag{12}$$

The next step of the synchrosqueezing requires us to obtain the preliminary frequencies according to Eq. (6). Since the Wx is a complex function, the partial derivative is calculated as the sum of the partial derivatives of its components. According to [24], for every function of shape $f(x) = a(x) + ib(x)$ the derivative can be calculated as:

$$\frac{\partial f}{\partial x} = \frac{\partial a}{\partial x} + \mathrm{i}\frac{\partial b}{\partial x}, \tag{13}$$

Let us focus on the real part of the partial derivative of $Wx(u)$ only:

$$\mathrm{Re}\left(\frac{\partial Wx(u)}{\partial u}\right)_{Analit} = -K\omega_0 \sin(u\omega_0). \tag{14}$$

Similarly, if the derivation is numerical, by using the central difference scheme of the second order:

$$\frac{\partial f(x)}{\partial x} = \frac{f(x+h) - f(x-h)}{2\,h}, \tag{15}$$

the real part of Eq. (12) can be obtained as:

$$\mathrm{Re}\left(\frac{\partial Wx}{\partial u}\right)_{Numer} = \frac{K\cos((u+\Delta u)\omega_0) - K\cos((u-\Delta u)\omega_0)}{2\Delta u} \tag{16}$$

$$\mathrm{Re}\left(\frac{\partial Wx}{\partial u}\right)_{Numer} = -K\frac{\sin(u\omega_0)\sin(\Delta u\omega_0)}{\Delta u} \tag{17}$$

As the numerical result Eq. (17) is not equal to the analytical Eq. (14), their ratio is:

$$\frac{\mathrm{Re}\left(\frac{\partial Wx}{\partial u}\right)_{Numer}}{\mathrm{Re}\left(\frac{\partial Wx}{\partial u}\right)_{Analit}} = \frac{\sin(\omega_0\Delta u)}{\omega_0\Delta u}. \tag{18}$$

A similar procedure can be repeated for the imaginary part, resulting in:

$$\frac{\mathrm{Im}\left(\frac{\partial Wx}{\partial u}\right)_{Numer}}{\mathrm{Im}\left(\frac{\partial Wx}{\partial u}\right)_{Analit}} = \frac{\sin(\omega_0\Delta u)}{\omega_0\Delta u}. \tag{19}$$

Since the ratio is the same for both parts of the complex number, according to Eq. (6), the same ratio also holds for the preliminary frequency:

$$\frac{\omega(u,s)_{Numer}}{\omega(u,s)_{Analit}} = \frac{\sin(\omega_0\Delta u)}{\omega_0\Delta u}. \tag{20}$$

The significance of Eq. (20) is in the error estimation of the preliminary frequency, which arises from the numerical differentiation. When the time interval Δu is close to zero, the ratio Eq. (20) comes close to 1 and the error vanishes. However, if the time discretization is not sufficiently dense, then the ratio Eq. (20) is less than 1 and an unwanted frequency shift can arise. As is clear from Eq. (7), synchrosqueezing relies on the reassignment of the CWT coefficients $s_k \to \omega_l$ when the following criterion is fulfilled:

$$|\omega(u,s_k)_{Numer} - \omega_l| \leq \frac{\omega_l - \omega_{l-1}}{2}. \tag{21}$$

The numerically obtained $\omega(u, s_k)_{Numer}$ is always smaller than the real $\omega(u, s_k)_{Analit}$. In the process of synchrosqueezing, the criterion Eq. (21) always rearranges the coefficients in time-frequency plane to a new frequency which is the closest to the $\omega(u, s_k)_{Numer}$. This way, the error of numerically obtained $\omega(u, s_k)_{Numer}$ gets expressed as a shift to lower frequencies. The admissible error may be a subject for individual application, but in general we define the maximum admissible error as half of a frequency bin or $\Delta\omega/2$. Consequently, the frequencies that correspond to the midpoint of a bin are shifted to the lower boundary of the same bin. With a constant bin width of $\Delta\omega$, the critical ratio occurs at the highest frequency bin:

$$\frac{\omega(u,s)_{Numer}}{\omega(u,s)_{Analit}} = \frac{\omega_{max} + \omega_{max-1}}{2\omega_{max}} \tag{22}$$

$$\frac{\sin(\omega_0 \Delta u)}{\omega_0 \Delta u} = 1 - \frac{\Delta\omega}{2\,\omega_{max}} \tag{23}$$

A second-order Taylor series is applied to the left-hand side of Eq. (23) to obtain:

$$1 - \frac{(\omega_0 \Delta u)^2}{6} = 1 - \frac{\Delta\omega}{2\,\omega_{max}}. \tag{24}$$

The terms can be rearranged in order to express the maximum value of Δu, which yields a frequency shift that is smaller than or equal to $\Delta\omega/2$:

$$\Delta u = \frac{1}{\omega_0}\sqrt{\frac{3\,\Delta\omega}{\omega_{max}}}. \tag{25}$$

A larger Δu than defined in (25) results in the frequency shift:

$$\omega_{shift} = \omega_{Analit} - \omega_{Numer}. \tag{26}$$

Considering the ratio Eq. (20), the expected frequency shift for a given time resolution is

$$\omega_{shift} = \frac{\omega_0\,\Delta u - \sin(\omega_0\,\Delta u)}{\Delta u}. \tag{27}$$

3.1 Correction of a frequency shift

As seen from Eq. (25), the required Δu is inversely proportional to the frequency of a signal. Since $\Delta u = T_{sig}/N$, where T_{sig} is the time of the signal and N is the number of sampling points. Δu can be decreased if sampling is the sampling frequency is increased. To completely annihilate the frequency shift, the sampling frequency as high as 100 times the observed frequency

might be required. This is far beyond the Nyquist theorem or physical requirements for damping identification and thus redundant. Because of this, we suggest numerical approach to reduce the shift. We suggest calculating $\omega(u,s)_{Numer}$ with a larger Δu than predicted in Eq. (25), thus eliminating any redundancy. This yields a predictable frequency-shift error Eq. (20) that will be corrected with the introduction of the coefficient $C(s)$:

$$\omega(u,s)_{Corrected} = C(s)\ \omega(u,s)_{Numer}. \tag{28}$$

To completely eliminate the frequency shift, the coefficient would have to be equal to:

$$C = \frac{\omega_0 \Delta u}{\sin(\omega_0 \Delta u)}. \tag{29}$$

The problem with defining $C(s)$ is its dependence on the unknown ω_0. For this reason, we are proposing three different approaches: *a)* a scale-dependent coefficient, *b)* a shifted coefficient and *c)* an autocorrelated frequency.

The scale-dependent coefficient method suggests calculating a coefficient that is dependent on the scale s:

$$C_1(s) = \frac{\frac{\eta}{s}\Delta u}{\sin(\frac{\eta}{s}\Delta u)}. \tag{30}$$

Here, it is assumed that $\omega_0 = \eta/s$, which corresponds to the ridge of the CWT. This means that for the s on the ridge, the value of $C_1(s)$ is exactly as desired. For the points that do not correspond to the ridge, the error of $C_1(s)$ increases the further away from the ridge we get, but at the same time the amplitude of the CWT at these points decreases, leading to good results (shown later). The frequency shift at the maximum vanishes, and the resulting synchrosqueezed transform is spread over a few frequency bands.

The shifted-coefficient method is based on the idea that according to Eq. (20) the approximation of ω_0 is known: $\omega(u,s)_{Numer}$. This estimation is smaller than ω_0. The resulting coefficient C_2 calculated with $\omega(u,s)_{Numer}$ is also smaller than desired. Therefore, the frequency shift is not entirely eliminated, but is significantly reduced:

$$C_2 = \frac{\omega(u,s)_{Numer}\,\Delta u}{\sin(\omega(u,s)_{Numer}\,\Delta u)}. \tag{31}$$

The autocorrelated-frequency method is based on the fact that for a simple harmonic signal Eq. (10), the preliminary frequency equals the frequency of the signal: $\omega_{Analit}(u,s) = \omega_0$ [12]. This fact, combined with Eq. (28) and Eq. (29), results in:

$$\omega_0 = \frac{\omega_0 \, \Delta u}{\sin(\omega_0 \, \Delta u)} \, \omega(u,s)_{Numer}. \tag{32}$$

In this case, there is no need for a correction coefficient. The ω_0 can be expressed directly and is therefore equal to the sought frequency $\omega_0 = \omega(u,s)_{corrected}$. The sought frequency can be expressed as:

$$\omega(u,s)_{corrected} = \frac{\sin^{-1}(\omega(u,s)_{Numer} \, \Delta u)}{\Delta u}. \tag{33}$$

4 Close Modes

Close modes are a common occurrence in vibrating systems with many degrees of freedom. They often arise as a result of symmetry or near symmetry in a given structure. In the case of close modes, the identification of the correct modal parameters can prove to be difficult.

On the one hand, as shown by Simonovski and Boltežar [25], the frequency spread of a Gabor wavelet can be expressed as:

$$\sigma_{\omega_{u,s}} = \frac{1}{s} \frac{1}{\sqrt{2}} \frac{1}{\sigma} \tag{34}$$

So for smaller parameters s and σ, the wavelet transform is spread over different frequencies, and in the case of noisy signals, the identification of close modes from a scalogram is made difficult.

Synchrosqueezing a wavelet transform nullifies the CWT's frequency spread by allocating the coefficients to a single frequency line. In this way, even when dealing with very close frequencies and using smaller parameters, σ and η, the SWT enables us to correctly identify the modes as separate.

The other problem occurring with close modes is beats. A signal with two harmonic frequencies Eq. (35) of constant and same amplitudes can also be seen as a signal of a single, average frequency with varying amplitude, see Eq. (36).

$$x(t) = A_0 \, \cos(\omega_{01} \, t) + A_0 \, \cos(\omega_{02} \, t), \tag{35}$$

$$x(t) = 2A_0 \, \cos\left(\frac{\omega_{01} - \omega_{02}}{2} \, t\right) \, \cos\left(\frac{\omega_{01} + \omega_{02}}{2} \, t\right), \tag{36}$$

Since the damping ratio is estimated from the logarithmic decline of the amplitudes along the ridge Eq. (9), any oscillation on the ridge makes the identification of the damping ratio less reliable, so beats must be avoided.

When calculating the SWT, the apparent time-wise oscillation of the amplitude introduced by the beats proves to be even more problematic than with the CWT. The re-allocation criterion used for the synchrosqueezing depends on the time-wise derivative of the CWT and the oscillation of the beats makes the criterion less reliable. Even in cases where the beats are negligible when using the CWT, the beats are expressed and this distorts the identification with the SWT.

Because of the aforementioned sharpening, the SWT is good for determining whether a given signal consists of a single mode or of two closely spaced modes. However, if the two modes are sufficiently close, the beating might occur. Beating greatly diminishes the SWT's capability of reliably extracting the damping ratio. For damping identification on signals where close modes might produce beating, the CWT is preferred to the SWT.

5 Modification of synchrosqueezing for damping identification

As shown by Montejo and Vidot-Vega [21], synchrosqueezing a CWT yields a sharper time-scale representation, but, on the other hand, when identifying damping ratios it is less stable than when using coefficients of the CWT.

The main reason for the instability of such an identification is the rearrangement of the individual CWT coefficients. In the case of a pure harmonic signal without any noise Eq. (10), all the values from the time-frequency plane are squeezed into a single line. But when the noise is taken into account, the squeezing becomes less stable. Instead of a single line, the synchrosqueezed transform is spread over several frequencies. However, unlike with the CWT, this frequency spread is not constant with time. For damping identification, the ridge and its skeleton have to be identified. Because of the re-assignment in synchrosqueezing, at different points along the ridge, a different number of CWT coefficients might have been summed into the ridge. Therefore, the amplitude of the skeleton is no longer proportional only to the amplitude of the vibration, but it is also dependent on the sychrosqueezing. In this way the noise error is increased and this represents the main reason why the synchrosqueezing CWT is less reliable than the CWT alone when dealing with noisy signals [21].

The identification procedure in Sec. 2.1 would be more reliable if the re-

assigning criterion in Eq. (7) was more stable. As described by Daubecies in [13], synchrosqueezing can be defined with an arbitrary reassigning rule. From the nature of a signal in a free-response dynamic system we know that each mode will change its amplitude, but its angular frequency will remain almost constant. Because of this, we developed two criteria that are not dependent on time: *a)* the average SWT and *b)* the proportional SWT.

The Average SWT criterion uses the average preliminary frequency $\omega_{avg}(s)$ instead of the preliminary frequency $\omega(u, s)$. The average preliminary frequency is a time-wise average of $\omega(u, s)$:

$$\omega_{avg}(s) = \frac{1}{N_u} \sum_{u_i} \omega(u_i, s). \tag{37}$$

N_u is a number of points in time. The synchrosqueezing is then carried out in the same way as originally, just with the new criterion:

$$_{Average}T(u, \omega_l) = (\Delta\omega)^{-1} \sum_{s_k : |\omega_{avg}(s_k) - \omega_l| \leq \Delta\omega/2} Wx(u, s_k)\, s_k^{-3/2} \Delta s. \tag{38}$$

The proportional SWT criterion is based on a similar idea, but rather than calculating a criterion and rearranging the entire frequency line into a single new frequency line, each line can be spread and rearranged into more than one different frequency bin.

Firstly, the preliminary frequencies are calculated following Eq. (6).

Secondly, focusing on a single frequency line s_k, the number of points N_u in time is counted. For each line s_k, the number of points N_l that correspond to each line l is counted:

$$N_u = |\{u \in s_k\}|, \tag{39}$$

$$N_l = |\{u \in s_k;\ |\omega(u, s_k) - \omega_l| \leq \Delta\omega/2\}|. \tag{40}$$

Thirdly, $\alpha_{prop,l}(s_k)$ is calculated as a fraction of the N_l number of points that correspond to any given frequency line and the number of all the points in time N_u:

$$\alpha_{prop,l}(s_k) = \frac{N_l}{N_u} \tag{41}$$

.

Finally, each element from a given line s_k is rearranged to the other lines in proportion to $\alpha_{prop,l}(s_k)$. For this, the synchrosqueezing is carried out

like originally, except that the summation is carried out over all frequencies and there is an added coefficient $\alpha_{prop,l}(s)$

$$_{Proportional}T(u,\omega_l) = (\Delta\omega)^{-1} \sum_{s_k} \alpha_{prop,l}(s)\, Wx(u,s_k)\, s_k^{-3/2} \Delta s. \quad (42)$$

6 Experiments

6.1 Frequency shift

To illustrate the problem and possible solutions from Section 3, a simple numerical experiment is carried out. A pure harmonic signal of a shape $x(t) = A_0 \cos(\omega_0 t)$ is generated.

Table 1: Parameters of a signal and CWT

Variable	Description	Value
A_0	Amplitude	1
ω_0 [rad/s]	Angular frequency	125.6
t [s]	Time	0 - 4
N	Number of discrete points	500
σ	Parameter σ	0.05
η [rad/s]	Frequency modulation	250
f [Hz]	Frequency range	10 - 25
Δf [Hz]	Frequency resolution	0.33

Given the parameters from Table 1 and according to Eq. (25), the time resolution should be $\Delta u = 0.0009$ s. To demonstrate the frequency shift and the effect of different correctional approaches from Section 3, a significantly larger $\Delta u = 0.008$ s is used. The expected frequency shift according to Eq. (27) is 3.2 Hz.

The results are presented in Figure 1, as a plot of a synchrosqueezed wavelet transform. Figure 1a) shows a standard transform that results in a frequency shift due to an inappropriate Δu. An original signal of 20 Hz is shifted to approximately 17 Hz.
Figure 1b) of the picture represents the same procedure, with an added attempt to eliminate the frequency shift with the use of the scale-dependent-coefficients correction Eq. (30). The result shows that the frequency error almost entirely vanishes, but at the same time, the resulting transform is spread over neighbouring frequencies.

Figure 1c) shows the effect of the shifted-coefficient method Eq. (31). As predicted, the frequency shift is reduced, but not eliminated. There is no effect on the sharpness of the result.
Figure 1d) shows the autocorrelated approach Eq. (33). This approach yields the best results, as it completely eliminates the frequency shift and does not affect the frequency spread of the transform.

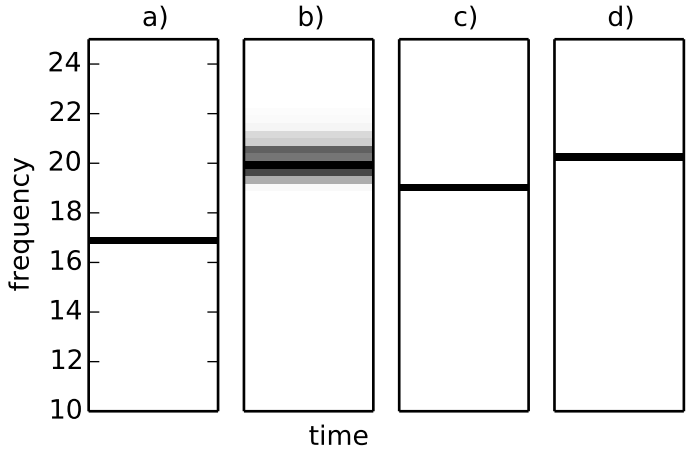

Figure 1: Frequency shift: a) without correction, b) scale-dependent coefficients, c) shifted coefficient, d) autocorrelated frequency

6.2 Noisy signals

This section aims to demonstrate the robustness of different methods when dealing with noisy signals. In order to obtain the different levels of noise while examining the same signal, the experiment will be carried out numerically. A signal is defined as:

$$x(t) = A_0 \cos(\omega_0 \sqrt{(1-\zeta^2)} t)\, \mathrm{e}^{-\zeta\, \omega_0\, t} + B_0\, O_{Noise} \tag{43}$$

The parameters used for this transform are given in Table 2.

O_{Noise} denotes the noise of the uniform distribution added to the signal, whereas B_0 is used to change its amplitude. This simulates the different levels of white noise that is often unavoidable when setting up an experiment. To describe the amount of noise, the signal-to-noise ratio (SNR) is used as defined in Eq. (44).

$$SNR = 20 \log_{10} \left(\frac{\sigma_{signal}}{\sigma_{noise}} \right) \tag{44}$$

Table 2: Parameters of a signal 43 and CWT

Variable	Description	Value
A_0	Amplitude of signal	1
B_0	Amplitude of noise	0.2 - 7
ω_0 [rad/s]	Angular frequency	125.6
t [s]	Time	0 - 2
ζ	Damping ratio	0.02
N	Number of discrete points	600
σ	Parameter σ	1.0
η [rad/s]	Frequency modulation	31,4
f [Hz]	Frequency range	15 - 25
Δf [Hz]	Frequency resolution	0.1
Δu [s]	Time resolution	0.0033

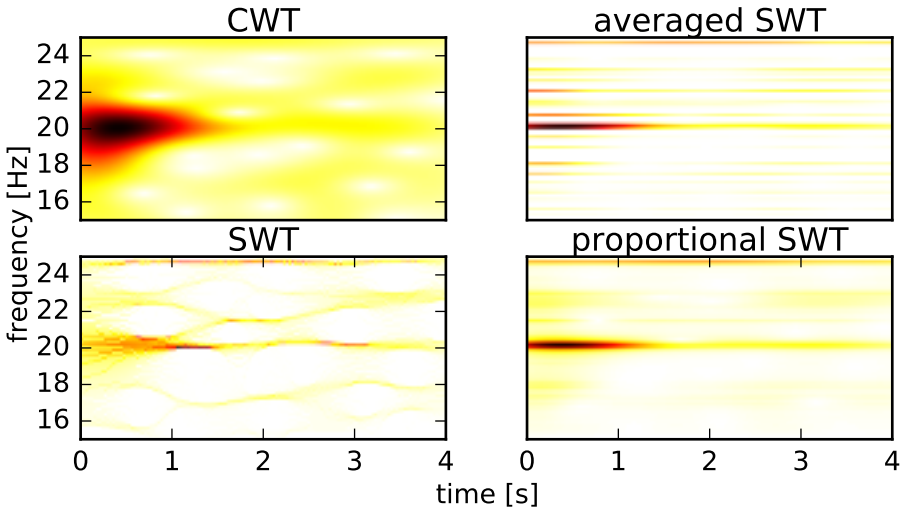

Figure 2: Time-frequency representations of the signal with SNR = -5 db using different transforms

σ_{signal} is the standard deviation of the signal, and σ_{noise} is the standard deviation of the noise. The standard deviation of a simple cosine wave with a constant amplitude equals: $\sigma(A_0 \cos \omega t) = A/\sqrt{2}$. For a given signal

Eq. (43) the standard deviation at time t equals:

$$\sigma_{signal} = \frac{A_0 \, \mathrm{e}^{-\zeta \omega_d t}}{\sqrt{2}} \tag{45}$$

It is assumed here that the origin of the noise is not directly dependent on the vibration itself, i.e., although the amplitude of the signal decreases over time, the amplitude of the noise remains unchanged.

$$\sigma_{noise} = \frac{B_0}{\sqrt{12}} \tag{46}$$

Because of this, the SNR increases over time. To obtain a single number, the average standard deviations of the signal and the noise are computed.

Because of the random nature of the added noise, 3000 signals of the form Eq. (43) are generated across different levels of noise. Each of them was then transformed with the CWT, the SWT, the averaged SWT and the proportional SWT. The damping ratio was extracted as described in Section 2.1. The extracted damping ratio is compared to the theoretical one from Table 2 and a realative error is calculated $err = |\zeta_{theoretical} - \zeta_{extracted}|/\zeta_{theoretical}$. The relative errors of the identified damping ratios are presented in Figure 3.

The results are consistent with the findings of [21] in that the pure SWT performs worse than the CWT at each noise level. Furthermore, it can be seen that the averaged SWT criterion and the proportional SWT criterion, as proposed in Section 5, do not exhibit the same problem as the SWT. The averaged SWT is as robust as the CWT for all levels of noise. At low and high levels of noise, the proportional SWT performs as well as the CWT, whereas for a SNR of approximately 0, the proportional SWT yields results with smaller errors than the CWT.

6.3 Application to real data

Both proposed modifications of the synchrosqueezed wavelet transform have also been applied to real data, where the CWT is used as a benchmark. The data comes from the free response of a 500-mm-long steel beam with a cross-section of 15 x 30 mm^2. Details of the setup can be found in [5]. The frequencies and the damping ratios for the first six natural frequencies were sought. The parameters for the frequencies and the damping identification can be found in Table 3.

The result for the first six natural frequencies and the corresponding damping ratios obtained with the CWT, the SWT with the averaged criterion and the SWT with the proportional criterion are presented in Table 4.

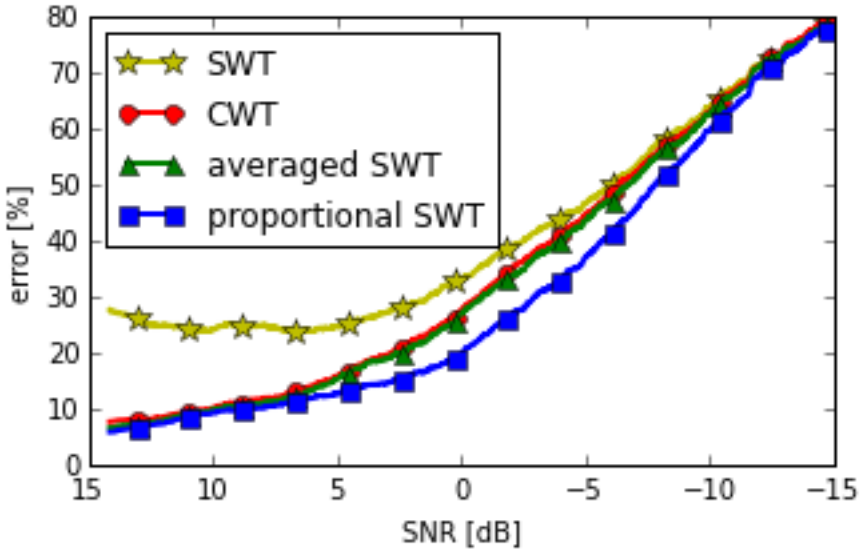

Figure 3: Relative errors of damping ratios identified from noisy signals using different transforms

Table 3: Parameters for different natural frequencies

Variable						
Natural freq.	1	2	3	4	5	6
N	300000	300000	300000	8192	8192	8192
σ	1.0	1.0	1.0	1.0	1.0	1.0
η [Hz]	25	100	200	300	500	500
f [Hz]	270-330	820-880	1600-1700	2700-2800	4000-4100	5550-5650
Δf [Hz]	1	1	1	1	1	1
t [s]	0 - 1.1	0 - 1.1	0 - 1.1	0 - 0.125	0 - 0.125	0 - 0.125
Δu [s]	3.3e-5	3.3e-5	3.3e-5	1.5 e-6	1.5 e-6	1.5 e-6

All the methods identified the same six natural frequencies, with the differences not exceeding 0.5 %. The identified damping ratios were also very similar. The damping ratios for the fifth and sixth natural frequencies are higher when identified using the SWT with modified criteria than when identified by the CWT. Nevertheless, the differences are smaller than the confidence interval usually associated with the damping identification of real

structures.

Table 4: Identified natural frequencies and damping ratios

Natural freq.	CWT freq. [Hz]	avg SWT freq. [Hz]	prop SWT freq. [Hz]	CWT ζ	avg SWT ζ	prop SWT ζ
1	310	310	310	1.29 e-4	1.29 e-4	1.29 e-4
2	849	849	849	1.78 e-4	1.78 e-4	1.78 e-4
3	1652	1651	1652	3.91 e-4	3.91 e-4	3.91 e-4
4	2749	2749	2749	9.30 e-4	9.32 e-4	9.32 e-4
5	4059	4054	4054	4.54 e-4	4.73 e-4	4.72 e-4
6	5590	5565	5566	6.32 e-4	7.21 e-4	6.75 e-4

7 Conclusion

When analyzing a signal with the CWT, a trade-off between localizing the signal in time and localizing it in terms of frequency is always present. With synchrosqueezing, a signal is always localized in frequency and the aforementioned trade-off no longer poses a challenge. Therefore, smaller σ and η can be used, which improves the time localisation and reduces the edge effect, while at the same time maintaining the frequency localization.

When calculating the SWT, calculating the preliminary frequencies is critical. We have shown that when calculating the preliminary frequencies using the central difference scheme, an error is obtained that shifts the SWT to lower frequencies. Three methods for correcting this shift are shown, of which the autocorrelated method works the best and nullifies the shift completely.

In the case of close modes, the SWT can help to distinguish between a single and two adjacent frequencies. When assessing close modes, beats may appear, which distorts the scalogram. In comparison to the CWT, the SWT is far more susceptible to beats, which makes the SWT less suitable for close-modes identification.

To deal with the weaknesses of the SWT in cases of close modes and noisy signals, two modifications to the SWT are proposed. Both are designed for constant frequencies of oscillation and are based on the time-wise averaging of the re-allocation criterion.

To validate the proposed modification, a numerical example was carried

out. It was shown that in the case of noisy signals, both the proportional and the averaged SWT perform better than the SWT, and as well as the CWT. In the region around SNR = 0 dB, the proportional SWT yields better results than the CWT.

Finally, the proposed modifications were tested on a real signal of the vibration of a uniform beam; they were consistent for both methods as well as for the CWT.

References

[1] WJ Staszewski. Identification of damping in mdof systems using time-scale decomposition. *Journal of sound and vibration*, 203(2):283–305, 1997.

[2] M Ruzzene, A Fasana, L Garibaldi, and B Piombo. Natural frequencies and dampings identification using wavelet transform: application to real data. *Mechanical Systems and Signal Processing*, 11(2):207–218, 1997.

[3] Hai Ping Yin and Pierre Argoul. Integral transforms and modal identification. *Comptes Rendus de l'Academie des Sciences Series IIB Mechanics Physics Astronomy*, 8(327):777–783, 1999.

[4] Claude-Henri Lamarque, Stéphane Pernot, and A Cuer. Damping identification in multi-degree-of-freedom systems via a wavelet-logarithmic decrement–part 1: Theory. *Journal of Sound and Vibration*, 235(3):361–374, 2000.

[5] Janko Slavič, Igor Simonovski, and Miha Boltežar. Damping identification using a continuous wavelet transform: application to real data. *Journal of Sound and Vibration*, 262(2):291–307, 2003.

[6] Miha Boltežar and Janko Slavič. Enhancements to the continuous wavelet transform for damping identifications on short signals. *Mechanical Systems and Signal Processing*, 18(5):1065–1076, 2004.

[7] Thien-Phu Le and Pierre Argoul. Continuous wavelet transform for modal identification using free decay response. *Journal of sound and vibration*, 277(1):73–100, 2004.

[8] Janko Slavič and Miha Boltežar. Damping identification with the morlet-wave. *Mechanical Systems and Signal Processing*, 25(5):1632–1645, 2011.

[9] Darren E Holland, Jason R Rodgers, and Bogdan I Epureanu. Measurement point selection and modal damping identification for bladed disks. *Mechanical Systems and Signal Processing*, 33:97–108, 2012.

[10] CA Gaviria and LA Montejo. Wavelet based damping identification-from noise contaminated signals. In *Proceedings of the 10th National Conference in Earthquake Engineering*, 2014.

[11] Hui Zhang, Jianmin Yang, and Longfei Xiao. Damping ratio identification using a continuous wavelet transform to vortex-induced motion of a truss spar. *Ships and Offshore Structures*, 9(6):596–604, 2014.

[12] Ingrid Daubechies, Jianfeng Lu, and Hau-Tieng Wu. Synchrosqueezed wavelet transforms: an empirical mode decomposition-like tool. *Applied and computational harmonic analysis*, 30(2):243–261, 2011.

[13] Ingrid Daubechies and Stephane Maes. A nonlinear squeezing of the continuous wavelet transform based on auditory nerve models. *Wavelets in medicine and biology*, pages 527–546, 1996.

[14] Shuai Shang, Liguo Han, Wei Hu, et al. Seismic data analysis using synchrosqueezing wavelet transform. In *2013 SEG Annual Meeting*. Society of Exploration Geophysicists, 2013.

[15] Chuan Li and Ming Liang. Time–frequency signal analysis for gearbox fault diagnosis using a generalized synchrosqueezing transform. *Mechanical Systems and Signal Processing*, 26:205–217, 2012.

[16] Zhipeng Feng, Xiaowang Chen, and Ming Liang. Iterative generalized synchrosqueezing transform for fault diagnosis of wind turbine planetary gearbox under nonstationary conditions. *Mechanical Systems and Signal Processing*, 52:360–375, 2015.

[17] B Hazra, A Sadhu, and S Narasimhan. Fault detection of gearboxes using synchro-squeezing transform. *Journal of Vibration and Control*, page 1077546315627242, 2016.

[18] Chuan Li, Vinicio Sanchez, Grover Zurita, Mariela Cerrada Lozada, and Diego Cabrera. Rolling element bearing defect detection using the generalized synchrosqueezing transform guided by time–frequency ridge enhancement. *ISA transactions*, 2015.

[19] Juanjuan Shi, Ming Liang, Dan-Sorin Necsulescu, and Yunpeng Guan. Generalized stepwise demodulation transform and synchrosqueezing for time–frequency analysis and bearing fault diagnosis. *Journal of Sound and Vibration*, 368:202–222, 2016.

[20] Dmytro Iatsenko, Peter VE McClintock, and Aneta Stefanovska. Linear and synchrosqueezed time-frequency representations revisited. *Digital Signal Processing*, 42(C):1–26, 2015.

[21] Luis A Montejo and Aidcer L Vidot-Vega. Synchrosqueezed wavelet transform for frequency and damping identification from noisy signals. *Smart Structures and Systems*, 9(5):441–459, 2012.

[22] Stephane Mallat. *A Wavelet Tour of Signal Processing*. Academic press, 1998.

[23] René Carmona, Wen L Hwang, Brun Torrésani, et al. Characterization of signals by the ridges of their wavelet transforms. *Signal Processing, IEEE Transactions on*, 45(10):2586–2590, 1997.

[24] D. Sarason. *Complex Function Theory*. American Mathematical Society., 2nd edition, 2007.

[25] Igor Simonovski and Miha Boltežar. The norms and variances of the gabor, morlet and general harmonic wavelet functions. *Journal of Sound and Vibration*, 264(3):545–557, 2003.